System Reliability Analysis with Second Order Saddlepoint Approximation

Hao Wu[1,2]

Graduate Research Assistant

1. Department of Mechanical and Energy Engineering

Indiana University - Purdue University Indianapolis,

723 W. Michigan Street

Indianapolis, IN, 46202, United States

2. School of Mechanical Engineering

Purdue University

West Lafayette, IN, 47907, United States

E-mail: wu1508@purdue.edu

Xiaoping Du

Professor

Department of Mechanical and Energy Engineering

Indiana University - Purdue University Indianapolis,

723 W. Michigan Street

Indianapolis, IN, 46202, United States

E-mail: duxi@iu.edu

Abstract

The second order saddlepoint approximation (SPA) has been used for component reliability analysis for higher accuracy than the traditional second order reliability method. This work extends the second order SPA to system reliability analysis. The joint distribution of all the component responses is approximated by a multivariate normal distribution. To maintain high accuracy of the approximation, the proposed method employs the second order SPA to accurately generate the marginal distributions of the component responses; to simplify computations and achieve high efficiency, the proposed method estimates the covariance matrix of the multivariate normal distribution with the first order approximation to the component responses. Examples demonstrate the high effectiveness of the second order SPA method for system reliability analysis.

1. INTRODUCTION

One of the criteria for systems design is to avoid system failures or minimize the probability of system failures. It is therefore necessary to predict system reliability accurately and efficiently during the design process [1]. System reliability is typically measured by the probability that the system fulfills its intended function without failures [2]. There are multiple components in the system, and each component may have multiple failure modes. Suppose the *i*-th failure model has a limit-state function given by

$$Y_i = g_i(\mathbf{X}) \quad (i = 1, ..., m) \tag{1}$$

where Y_i is a component response, and $\mathbf{X}$ is the vector of random variables. If $Y_i < 0$, the failure model does not occur; otherwise, the failure mode occurs. If we consider a failure model as a component, component reliability is then computed by

$$R_i = \Pr(g_i(\mathbf{X}) < 0) = \int_{\Omega_i} f(\mathbf{x})d\mathbf{x} \quad (i = 1, 2, ..., m) \tag{2}$$

where Ω_i is the component safe domain or the domain defined by $\{\mathbf{X} : Y_i = g_i(\mathbf{X}) < 0\}$, and $f(\mathbf{x})$ is the joint probability density function (PDF) of $\mathbf{X}$. For a series system, if one failure mode occurs, the system fails. System reliability is therefore given by

$$R_S = \Pr\left(\bigcap_{i=1}^{m} g_i(\mathbf{X}) < 0\right) = \int \cdots \int_{\Omega_S} f_{\mathbf{X}}(\mathbf{x})d\mathbf{x} \tag{3}$$

where Ω_S is the system safe domain or the domain defined by $\left\{\mathbf{X} : \bigcap_{i=1}^{m} g_i(\mathbf{X})\right\} < 0$, and m is the number of components in the system.

In practice, it is difficult to integrate a multidimensional PDF over the safe domain in Eq. (3). Different approaches have therefore been developed to approximate the multi-dimensional integral. They include the bound approximation, surrogate approaches, and analytical approaches.

Bound approximation methods predict system reliability with lower and upper bounds. The first order bound method for series systems assumes that all the component responses are completely dependent or mutually exclusive. Based on this assumption, upper and lower bounds are derived. Ditlevsen [3] developed the second-order bound method by taking into account all the single mode failure probabilities and all the pairwise mode intersection failure probabilities to narrow the first order bound. Song and Der Kuireghian [4] proposed a linear programming (LP) method to compute the system reliability bound. The LP bounds are independent of the ordering of the components and are guaranteed to produce the narrowest possible bounds. Another reliability bound method is the complementary intersection method [5]. It approximates the reliability of series systems with eigenvector dimension reduction and produces more accurate results compared with the first and the second order bound methods. More studies on system reliability bound methods can be found in Refs. [6, 7].

Surrogate approaches predict single-valued system reliability by creating surrogate models for component responses and using Monte Carlo simulation (MCS). Surrogate models are created first, and then system reliability is estimated with MCS based on the surrogate models. The surrogate modeling methods include the polynomial chaos expansion (PCE) [8], Support Vector Machine

(SVM) [9], and Kriging method [10-13]. The recent development in this area is to perform surrogate modeling and MCS simultaneously. For example, Bichon et al. [10, 11] applied the efficient global optimization to reliability assessment. This method uses the active learning function called the Expected Feasibility Function (EFF) to choose new training points in the vicinity of the limit state, resulting in building an accurate surrogate model with fewer function evaluations. Fauriat and Gayton [12] proposed to build the initial Kriging surrogate model and continually refine the model by choosing new training points from a pre-sampled MCS population. Wu and Du proposed a new kriging method to predict system reliability that combines MCS and the Kriging method with improved accuracy and efficiency[13].

Analytical methods use neither surrogate models nor MCS and also produce single-valued system reliability. They approximate nonlinear limit-state functions so that the system probability integral can be easily computed. The methods include the use of the First Order Reliability Method (FORM) [14, 15], Second Order Reliability Method (SORM) [16, 17], and Saddlepoint Approximation Method (SPA) [15, 18]. FORM is the most well-known method due to its good balance between accuracy and efficiency. It at first transforms random variables into standard normal variables and then it identifies the reliability index, which is the minimum distance from the origin to the linearized and transformed limit-state function at the most probable point (MPP). System reliability is then approximated by the multidimensional integration of the joint probability density function after the marginal distributions and correlation coefficients of component states are obtained by the first order approximation [14, 19]. Although the efficiency of such method is good, the accuracy may not be good if limit-state functions are highly nonlinear. Therefore, Madsen [17] presented an extension of FORM based on a more accurate approximation of the limit-state function, and the result shows smaller differences between the second order approximation and the exact result.

Among the above methods, SPA can improve accuracy for problems with or without the non-normal to normal transformation. Du estimated the system reliability by SPA without any transformation on random input variables, leading to more accurate result than the FORM [6]. But the method is still the first order approximation and produces bounds of system reliability. An extension of the first order SPA to the second order SPA on component reliability analysis has also been proposed to accommodate quadratic functions, and the method is more accurate than the first order SPA and SORM without sacrificing computational efficiency [20]. Papadimitriou et al. proposed a new mean-value second-order saddlepoint approximation method for reliability analysis of nonlinear systems with correlated non-Gaussian and multimodal random variables, and the result is more accurate than FORM and SORM [21]. But these methods are for only the component reliability analysis.

The purpose of this work is to extend the second-order SPA to system reliability analysis in order to achieve high accuracy. The joint distribution of all the component responses is approximated by a multivariate normal distribution. The second order SPA is used to approximate the marginal distributions of the component responses for higher accuracy. The covariance matrix of the multivariate normal distribution is estimated using the first order approximation.

The second-order SPA for component reliability analysis is briefly reviewed in Section 2. The extension of the second-order SPA to system reliability analysis is discussed in Section 3 followed by examples in Section 4. Conclusions are made in Section 5.

2. REVIEW OF SECOND ORDER SPA

In this section, we review the second order SPA for component reliability analysis [20]. It is the basis of the proposed system reliability method in this work.

2.1 MPP search

The method first approximates the limit-state function with a second order polynomial. It is the same approximation in the original SORM [22], which involves the MPP search in the standard normal space using FORM. With the assumption that all variables in $\mathbf{X}$ are independent, they are transformed into the standard normal variables **U**. The transformation is given by

$$F_i(X_i) = \Phi(U_i) \tag{4}$$

where $F_i(\cdot)$ and $\Phi(\cdot)$ are the cumulative distribution functions (CDFs) of X_i and U_i, respectively. Then the transformed standard normal variables are

$$U_i = \Phi^{-1}[F_i(X_i)] \tag{5}$$

After the transformation, the limit state function becomes

$$Y = g(\mathbf{X}) = G(\mathbf{U}) \tag{6}$$

Then, the minimum distance from the original to the limit-state surface $G(\mathbf{U}) = 0$ is identified. The distance is the reliability index β. The minimum distance point is called the MPP. The model for searching for the MPP is given by

$$\begin{cases} \min \|\mathbf{u}\| \\ \text{subject to} \quad G(\mathbf{u}) = 0 \end{cases} \tag{7}$$

where $\|\cdot\|$ means the length of a vector, namely

$$\beta = \|\mathbf{u}\| = \sqrt{u_1^2 + u_2^2 + \cdots u_n^2} = \sum_{i=1}^{n} u_i^2 \tag{8}$$

The solution from Eq. (7) is the MPP $\mathbf{u}^* = (u_1^*, u_2^*, ..., u_n^*)$.

2.2 Quadratic limit-state function

After the MPP is found, the limit-state function is approximated by

$$Q(\mathbf{U}) = \frac{1}{2}(\mathbf{u}^*)^{\mathrm{T}} \nabla^2 G(\mathbf{u}^*)\mathbf{u}^* - \nabla G(\mathbf{u}^*)^{\mathrm{T}} \mathbf{u}^* + \left(\nabla G(\mathbf{u}^*) - \nabla^2 G(\mathbf{u}^*)\mathbf{u}^*\right)^{\mathrm{T}} \mathbf{U} + \frac{1}{2}\mathbf{U}^{\mathrm{T}} \nabla^2 G(\mathbf{u}^*)\mathbf{U} \tag{9}$$

where $\nabla G(u^*) = \left(\frac{\partial G}{\partial U_1}\bigg|_{\mathbf{u}^*}, ..., \frac{\partial G}{\partial U_n}\bigg|_{\mathbf{u}^*} \right)$ is the gradient, and $\nabla^2 G(\mathbf{u}^*)$ is the Hessian matrix, given by

$$\nabla^2 G(\mathbf{u}^*) = \begin{bmatrix} \frac{\partial^2 G}{\partial U_1^2} & \frac{\partial^2 G}{\partial U_1 U_2} & \cdots & \frac{\partial^2 G}{\partial U_1 U_n} \\ \frac{\partial^2 G}{\partial U_2 U_1} & \frac{\partial^2 G}{\partial U_2^2} & \cdots & \frac{\partial^2 G}{\partial U_2 U_n} \\ \vdots & \vdots & \ddots & \vdots \\ \frac{\partial^2 G}{\partial U_n U_1} & \frac{\partial^2 G}{\partial U_n U_2} & \cdots & \frac{\partial^2 G}{\partial U_n^2} \end{bmatrix}_{\mathbf{u}^*} \tag{10}$$

The independent standard normal vector $\tilde{\mathbf{U}} = (\tilde{U}_1, \tilde{U}_2, ..., \tilde{U}_n)$ can be easily generated as follows:

$$\tilde{\mathbf{U}} = \mathbf{D}^{-1}\mathbf{U} \tag{11}$$

where $\mathbf{D}$ is an orthogonal matrix whose column vectors are the eigenvectors of $\frac{1}{2}\nabla^2 G(\mathbf{u}^*)$, and $\tilde{\mathbf{U}} = (\tilde{U}_1, \tilde{U}_2, ..., \tilde{U}_n)$ is a vector of independent standard normal random variables.

Thus, Eq. (9) is expressed in the form of a quadratic polynomial function, as follows:

$$Q(\tilde{\mathbf{U}}) = a + \tilde{\mathbf{b}}^{\mathrm{T}}\tilde{\mathbf{U}} + \tilde{\mathbf{U}}^{\mathrm{T}}\tilde{\mathbf{C}}\tilde{\mathbf{U}} \tag{12}$$

in which

$$\begin{cases} a = \frac{1}{2}(\mathbf{u}^*)^{\mathrm{T}}\nabla^2 G(\mathbf{u}^*)\mathbf{u}^* - \nabla G(\mathbf{u}^*)^{\mathrm{T}}\mathbf{u}^* \\ \tilde{\mathbf{b}} = \mathbf{D}^{\mathrm{T}}\mathbf{b} = (\tilde{b}_1, \tilde{b}_2, ..., \tilde{b}_n) \\ \tilde{\mathbf{C}} = \mathbf{D}^{\mathrm{T}}\mathbf{C}\mathbf{D} = diag(\tilde{c}_1, \tilde{c}_2, ..., \tilde{c}_n) \end{cases} \tag{13}$$

Since $\tilde{\mathbf{C}}$ is diagonal, Eq. (12) can be written as sum of quadratic functions of different standard normal variables.

$$Q(\mathbf{U}) = \sum_{i=1}^{n} Q_i(\tilde{\mathbf{U}}) = \sum_{i=1}^{n} (\tilde{a}_i + \tilde{b}_i\tilde{U}_i + \tilde{c}_i\tilde{U}_i^{\,2}) \tag{14}$$

where

$$\tilde{a}_i = \frac{a}{n} \tag{15}$$

and n is the total number of random variables.

$Q_i(\tilde{\mathbf{U}})$ is further rewritten as follows

$$Q_i(\tilde{\mathbf{U}}) = \begin{cases} (\sqrt{\tilde{c}_i}\tilde{U}_i + \dfrac{\tilde{b}_i}{2\sqrt{\tilde{c}_i}})^2 + \tilde{a}_i - \dfrac{\tilde{b}_i^2}{4\tilde{c}_i} \\ -(\sqrt{-\tilde{c}_i}\tilde{U}_i - \dfrac{\tilde{b}_i}{2\sqrt{-\tilde{c}_i}})^2 + \tilde{a}_i - \dfrac{\tilde{b}_i^2}{4\tilde{c}_i} \\ \tilde{a}_i + \tilde{b}_i\tilde{U}_i \end{cases} = \begin{cases} Z_i^2 + d_i & \tilde{c}_i > 0 \\ -Z_i^2 + d_i & \tilde{c}_i < 0 \\ \tilde{a}_i + \tilde{b}_i\tilde{U} & \tilde{c}_i = 0 \end{cases} \tag{16}$$

where d_i is constant and is determined by the following equation

$$d_i = \tilde{a}_i - \frac{\tilde{b}_i^2}{4\tilde{c}_i} \tag{17}$$

Z_i is obtained by a linear transformation of $\tilde{U}_i$

$$\begin{cases} Z_i = \sqrt{\tilde{c}_i}\tilde{U}_i + \dfrac{\tilde{b}_i}{2\sqrt{\tilde{c}_i}} & \tilde{c}_i > 0 \\ Z_i = \sqrt{-\tilde{c}_i}\tilde{U}_i - \dfrac{\tilde{b}_i}{2\sqrt{-\tilde{c}_i}} & \tilde{c}_i < 0 \end{cases} \tag{18}$$

Z_i is normally distributed and is denoted by $Z_i \sim N(\mu_{Z_i}, \sigma_{Z_i})$, where the mean μ_{Z_i} is given by

$$\mu_{Z_i} = \begin{cases} \dfrac{\tilde{b}_i}{2\sqrt{\tilde{c}_i}} & \tilde{c}_i > 0 \\ -\dfrac{\tilde{b}_i}{2\sqrt{-\tilde{c}_i}} & \tilde{c}_i < 0 \end{cases} \tag{19}$$

and the standard deviation σ_{Z_i} is given by

$$\sigma_{Z_i} = \begin{cases} \sqrt{\tilde{c}_i} & \tilde{c}_i > 0 \\ \sqrt{-\tilde{c}_i} & \tilde{c}_i < 0 \end{cases} \tag{20}$$

$V_i = (Z_i / \sigma_{Z_i})^2$ follows a noncentral chi-square distribution with freedom of 1 [23, 24];

namely $V_i \sim \chi^2(1,\lambda)$, where λ is a non-centrality parameter and given by

$$\lambda = (\frac{\mu_{Z_i}}{\sigma_{Z_i}})^2 \tag{21}$$

The limit-state function in Eq. (16) in finally expressed by a linear combination of either noncentral chi-square variables or standard normal variables.

$$\mathrm{Q}_i(\tilde{\mathbf{U}}) = \begin{cases} \sigma_{Z_i}^2 V_i + d_i & \tilde{c}_i > 0 \\ -\sigma_{Z_i}^2 V_i + d_i & \tilde{c}_i < 0 \\ \tilde{a}_i + \tilde{b}_i \tilde{U}_i & \tilde{c}_i = 0 \end{cases} \tag{22}$$

2.3 Saddlepoint approximation

Saddlepoint approximation is used to recover a PDF from its cumulant generating function (CGF). The CGF of the noncentral chi-square V_i in Eq. (22) is given by

$$K_{V_i}(t) = \frac{\lambda_i t}{1-2t} - \frac{1}{2}\log(1-2t) \tag{23}$$

The CGF of the standard normal variable $\tilde{U}_i$ in Eq. (22) is given by

$$K_{\tilde{U}_i} = \frac{1}{2}t^2 \tag{24}$$

The CGF of $Q_i(\tilde{\mathbf{U}})$ in Eq. (22) is then given by

$$K_{Q_i}(t) = \begin{cases} \dfrac{\lambda_i \sigma_{Z_i}^2 t}{1-2\sigma_{Z_i}^2 t} - \dfrac{1}{2}\log(1-2\sigma_{Z_i}^2 t) + d_i t & \tilde{c}_i > 0 \\ -\dfrac{\lambda_i \sigma_{Z_i}^2 t}{1+2\sigma_{Z_i}^2 t} - \dfrac{1}{2}\log(1+2\sigma_{Z_i}^2 t) + d_i t & \tilde{c}_i < 0 \\ \tilde{a}t + \dfrac{1}{2}b_i^2 t^2 & \tilde{c}_i = 0 \end{cases} \tag{25}$$

With all the above CGFs available, the CGF of the limit-state function in Eq. (12) $\mathrm{Q}(\tilde{\mathbf{U}})$ is then computed by

$$K_Q(t) = \sum_{i=1}^{n} K_{Q_i}(t) \tag{26}$$

After the CGF $K_Q(t)$ is obtained, it is straightforward to find the PDF of the limit-state function, and this requires to find the saddlepoint t_s, which is found by solving the following equation

$$K_Q^{'}(t) = 0 \tag{27}$$

where $K_Q^{'}(t)$ is the first derivative of $K_Q(t)$. According to the Lugannani and Rice's formula [25], the component reliability R_{SPA} is computed by

$$R_{\text{SPA}} = \Pr\{Q(\tilde{\mathbf{U}}) < 0\} = \Phi(w) + \phi(w)(\frac{1}{w} - \frac{1}{v}) \tag{28}$$

where $\Phi(\cdot)$ and $\phi(\cdot)$ are CDF and PDF of a standard normal distribution, respectively.

$$w = \text{sgn}(t_s)\{2[-K_Q(t_s)]\}^{1/2} \tag{29}$$

$$v = t_s[K_Q^{"}(t_s)]^{1/2} \tag{30}$$

where $\text{sgn}(t_s) = +1, -1 \text{ or } 0$, depending on whether t_s is positive, negative or zero; $K_Q^{"}(t)$ is the second derivative of $K_Q(t)$ with respect to *t*.

3. SYSTEM RELIABILITY WITH SECOND ORDER SPA

In this section, we discuss the new second-order SPA method for system reliability analysis. We focus on only series systems; the method, however, can also be extended to parallel systems and the combination of series and parallel systems.

System reliability can be estimated by integrating the joint PDF of all the input random variables in the safe region as indicated Eq. (3). To use SPA, we consider the PDF of component responses directly. The system state is determined by component responses predicted from component limit-state functions $Y_i = g_i(\mathbf{X})\ (i = 1, 2, ..., m)$. System reliability is then computed by

$$R_S = \Pr\left(\bigcap_{i=1}^{m} Y_i = g_i(\mathbf{X}) < 0,\ i = 1, 2, \ldots, m\right) \tag{31}$$

Eq. (31) requires the joint distribution of $Y_i\ (i = 1, 2, ...m)$. This means that we need to consider both component reliability and dependencies between component responses. Hereby, we approximate the joint distribution of all the component responses as a multivariate normal distribution.

If we consider only the first order terms of Eq. (9), the component limit-state function becomes

$$Q_i(\mathbf{U}) = -\nabla G(\mathbf{u}_i^*)^{\mathrm{T}} \mathbf{u}_i^* + \nabla G_i(\mathbf{u}_i^*)\mathbf{U} \tag{32}$$

If we divide both sides of Eq. (32) by the magnitude of the gradient, we obtain

$$\frac{Q_i(\mathbf{U})}{\left\|\nabla G(\mathbf{u}_i^*)\right\|} = -\frac{\nabla G(\mathbf{u}_i^*)^{\mathrm{T}}}{\left\|\nabla G(\mathbf{u}_i^*)\right\|}\mathbf{u}_i^* + \frac{\nabla G_i(\mathbf{u}_i^*)}{\left\|\nabla G(\mathbf{u}_i^*)\right\|}\mathbf{U} \tag{33}$$

Or

$$\frac{Q_i(\mathbf{U})}{\left\|\nabla G(\mathbf{u}_i^*)\right\|} = -\beta_i + \boldsymbol{\alpha}_i \mathbf{U} \tag{34}$$

The event of the safe component $Q_i(\mathbf{U}) < 0$ is equivalent to the event $-\beta_i + \boldsymbol{\alpha}_i \mathbf{U} < 0$. We then define a new variable

$$Z_i = -\beta_i + \boldsymbol{\alpha}_i \mathbf{U} \tag{35}$$

where $\boldsymbol{\alpha}_i$ is the directional vector and is given by

$$\boldsymbol{\alpha}_i = \frac{\nabla G_i(\mathbf{u}_i^*)}{\left\|\nabla G(\mathbf{u}_i^*)\right\|} = \frac{\mathbf{u}_i^*}{\beta_i} \tag{36}$$

We call Z_i an equivalent component response. It is obvious that Z_i follows a normal distribution. As a result, all the equivalent component responses follow a multivariate normal distribution.

System reliability is then approximated by

$$R_S = \Pr\left(\bigcap_{i=1}^{m} Q_i(\mathbf{U}) < 0\right) = \Pr\left(\bigcap_{i=1}^{m} \boldsymbol{\alpha}_i \mathbf{U} - \beta_i < 0\right) = \Pr\left(\bigcap_{i=1}^{m} Z_i < 0\right) \tag{37}$$

The multivariate normal distribution is denoted by $N(\boldsymbol{\mu}_Z, \boldsymbol{\Sigma}_Z)$, where $\boldsymbol{\mu}_Z$ is the mean vector of $\mathbf{Z} = (Z_1, Z_2, \ldots, Z_m)$ and $\boldsymbol{\Sigma}_Z$ is the covariance matrix. System reliability thus becomes the CDF $\Phi_m(\mathbf{0}; \boldsymbol{\mu}_Z, \boldsymbol{\Sigma}_Z)$ of $\mathbf{Z}$ at $\mathbf{0}$; namely

$$R_S = \Phi_m(\mathbf{0}; \boldsymbol{\mu}_Z, \boldsymbol{\Sigma}_Z) = \int_{-\infty}^{0} \ldots \int_{-\infty}^{0} f_Z(\mathbf{z}) d\mathbf{z} \tag{38}$$

where $f_Z(\mathbf{z})$ is the joint PDF of $\mathbf{Z}$.

Since we use the first approximation directly as indicated in Eq. (9), the method we have just discussed is the existing FORM for system reliability analysis.

The accuracy of the multivariate normal integration in Eq. (38) is closely related to the accuracy of the mean vector $\boldsymbol{\mu}_Z$ and covariance matrix $\boldsymbol{\Sigma}_Z$. In addition to high accuracy, we would also like to maintain high efficiency. There are mainly two ways to make the integration accurate and efficient. First, we improve the accuracy by determining $\boldsymbol{\mu}_Z$ with the second order component reliability obtained from the second order SPA. This strategy is adapted from Ref. [26] where the traditional SORM is used. Since the second-order SPA is in general more accurate than the traditional SORM, the new method has higher accuracy. We use the second order SPA to approximate the marginal CDF of Z_i at 0, which is the component reliability

$$F_{Z_i}(\mathbf{0}) = \Pr(Z_i < 0) = R_{\text{SPA}i} \tag{39}$$

where $R_{\text{SPA}i}$ is calculated by the second-order SPA method given in Eq. (28). Then the associated reliability index is determined by

$$R_{\text{SPA}i} = \Phi\left(\beta_i^{\text{SPA}}\right) \tag{40}$$

We call β_i^{SPA} an equivalent reliability index, which is given by

$$\beta_i^{\text{SPA}} = \Phi^{-1}\left(R_{\text{SPA}i}\right) \tag{41}$$

Since β_i^{SPA} is obtained from a more accurate reliability estimate, we use it to replace β_i in Eq. (35), resulting in $Z_i = -\beta_i^{\text{SPA}} + \boldsymbol{\alpha}_i \mathbf{U}$. The mean vector of the multivariable distribution of $\mathbf{Z}$ is then obtained.

$$\boldsymbol{\mu}_Z = (\beta_1^{\text{SPA}}, \beta_2^{\text{SPA}}, \ldots, \beta_m^{\text{SPA}}) \tag{42}$$

The above treatment ensures that the component reliability or the marginal distributions of component responses are accurately estimated by the second order approximation.

In order to simplify computations and achieve high efficiency, we use the same strategy in Ref. [26] to estimate the covariance matrix $\boldsymbol{\Sigma}_Z$. The idea is to use the first order approximation in Eq. (32). Let the components of $\boldsymbol{\Sigma}_Z$ be $\rho_{ij},\ i, j = 1, 2, \ldots, m,\ i \neq j$. The covariance is given by

$$\rho_{ij} = \boldsymbol{\alpha}_i^{\mathrm{T}} \boldsymbol{\alpha}_j \tag{43}$$

Then $\boldsymbol{\Sigma}_Z$ is given by

$$\boldsymbol{\Sigma}_Z = \begin{bmatrix} 1 & \rho_{12} & \cdots & \rho_{1m} \\ \rho_{21} & 1 & \cdots & \rho_{2m} \\ \vdots & \vdots & \rho_{ij} & \vdots \\ \rho_{m1} & \rho_{m2} & \cdots & 1 \end{bmatrix}_{m \times m} \tag{44}$$

The joint distribution of all component responses is now approximated by a multivariate normal distribution. With $\boldsymbol{\mu}_Z$ and $\boldsymbol{\Sigma}_Z$ available, the joint PDF of $\mathbf{Z} = (Z_1, Z_2, ..., Z_m)$ is expressed as

$$f_Z(\mathbf{z}) = \frac{1}{\sqrt{(2\pi)^m |\boldsymbol{\Sigma}_Z|}} \exp\left(-\frac{1}{2}(\mathbf{z} - \boldsymbol{\mu}_Z)^{\mathrm{T}} \boldsymbol{\Sigma}^{-1} (\mathbf{z} - \boldsymbol{\mu}_Z)\right) \tag{45}$$

Then system reliability R_S can be easily calculated by integrating the PDF in Eq. (38) from $(-\infty, ..., -\infty)$ to $(0, ..., 0)$ and the system probability of failure is

$$p_{Sf} = 1 - R_S \tag{46}$$

Many algorithms are available for integrating $f_Z(\mathbf{z})$ in Eq. (45) such as the first order multi-normal approximation (FOMN) [27], the product of conditional marginal method (PCM) [28], and Alan Genz method [29].

The proposed method provides a new way to estimate the system reliability with nonlinear limit-state functions. The dependencies between component responses are automatically accommodated in the system covariance matrix, and component marginal CDFs can be obtained accurately by using the second-order SPA. Thus this method not only achieves high accuracy in estimating system reliability but also simplifies the computations while maintaining high efficiency.

The procedure of the system reliability analysis with the second-order SPA is briefly summarized below.

(1) Transform random variable **X** into **U** in the standard normal space.

(2) Search for MPPs $\mathbf{u}_i^*$; obtain the reliability index β_i and first and second derivatives of component limit-state functions at the MPPs.

(3) Perform the second-order SPA for all components.

(4) Use SPA results to find the means of equivalent component responses.

(5) Use MPPs and reliability indexes to find the covariance matrix.

(6) Form the multivariate normal PDF and integrate it to obtain system reliability.

4 EXAMPLES

In this section, four examples are presented. The first example is used to demonstrate the proposed method while the other three examples show possible engineering applications. The accuracy is measured by the percentage error with respect to a solution from MCS. The error is calculated by

$$\varepsilon = \frac{\left| p_{\mathrm{S}f} - p_{\mathrm{S}f}^{\mathrm{MCS}} \right|}{p_{\mathrm{S}f}^{\mathrm{MCS}}} \times 100\% \tag{47}$$

where $p_{\mathrm{S}f}^{\mathrm{MCS}}$ and $p_{\mathrm{S}f}$ are probabilities of system failure from MCS and second order SPA method, FORM method or SORM method, respectively.

4.1 Example 1

The first example is mathematical example. A system consists of two physical components, and each component has one limit-state function. There are two basic random variables denoted by $\mathbf{X} = (X_1, X_2)$. X_1 is normally distributed with mean $\mu_1 = 4$ and standard deviation $\sigma_1 = 0.7$, and the distribution is denoted by $X_1 \sim N(4, 0.7)$. X_2 is lognormally distributed with mean $\mu_2 = 4$ and standard deviation $\sigma_2 = 1$, and the distribution is denoted by $X_2 \sim LN(4,1)$. The two limit-state functions are given by

$$g_1(\mathbf{X}) = 5 - X_1 X_2 \tag{48}$$

$$g_2(\mathbf{X}) = -X_1^2 - X_2^2 - 7X_1 + 16X_2 - 40 \tag{49}$$

At first, MPPs, reliability indexes, and directional vectors of the two limit-state functions are obtained. The results are given in Table 1.

Table 1 MPP, reliability index and directional vector

Place Table 1 here

Next, the reliability of each component is calculated by the second-order SPA with $R_1 = 0.9995$ and R_2=0.9994. The mean values of the two equivalent component responses $\mathbf{Z} = (Z_1, Z_2)$ are then calculated by

$$\boldsymbol{\mu}_Z = \boldsymbol{\beta}^{\mathrm{SPA}} = (\beta_i^{\mathrm{SPA}})_{i=1,2} = (\Phi^{-1}(R_i))_{i=1,2} = (3.3083, 3.2358)$$

The correlation coefficients ρ_{ij} are calculated by Eq. (43). For example, $\rho_{12} = \boldsymbol{\alpha}_1 \boldsymbol{\alpha}_2^{\mathrm{T}} = 0.3007$. Therefore, the covariance matrix is obtained.

$$\boldsymbol{\Sigma}_Z = \begin{bmatrix} 1 & \rho_{12} \\ \rho_{21} & 1 \end{bmatrix} = \begin{bmatrix} 1 & 0.3007 \\ 0.3007 & 1 \end{bmatrix}$$

Using Eq. (38), we obtain the system probability of failure $p_{Sf} = 1 - R_S = 1.0702 \times 10^{-3}$.

When FORM and SORM are used, the covariance matrices are the same as $\boldsymbol{\Sigma}_Z$, and the mean values of the two equivalent component responses are $\boldsymbol{\mu}_Z = \boldsymbol{\beta}^{\mathrm{FORM}} = (3.3620, 3.1450)$ and $\boldsymbol{\mu}_Z = \boldsymbol{\beta}^{\mathrm{SORM}} = (3.3086, 3.2274)$ Based on Eq. (38), the system probabilities of failure based on FORM and SORM are $p_{Sf} = 1.2111 \times 10^{-3}$ and $p_{Sf} = 1.0878 \times 10^{-3}$ respectively.

For MCS, a large sample size of 10^7 is used to compute the system reliability. All results are listed in Table 2, which shows that the errors of SOSPA, SORM and FORM are 0.289%, 1.35% and 12.% respectively. The results indicate that SOSPA is more accurate than FORM and SORM. The number of function calls in Table 2 indicate that FORM is more efficient than SOSPA and SORM. 1.0878×10^{-3}

Table 2 Probability of system failure in Example 1

Place Table 2 here

4.2 Example 2

Example 2 is an engineering example. Consider a roof structure [30], whose top boom and compression bars are made by concrete, while the bottom boom and all the tension bars are made of steel. Assume the bars bear a uniformly distributed load *q*. Let A_C and E_C be the cross sectional area and elastic modulus of the concrete bars, respectively. Let A_S and E_S be the cross sectional area and elastic modulus of the steel bars, respectively. The perpendicular deflection of the roof peak node *C* is calculated by

$$\Delta C = \frac{ql^2}{2}\left(\frac{3.81}{A_C E_C} + \frac{1.13}{A_S E_S}\right) \tag{52}$$

A failure event occurs when the perpendicular deflection ΔC exceeds 1.5 cm. The limit-state function is then defined by

$$g_1(\mathbf{X}) = \frac{ql^2}{2}\left(\frac{3.81}{A_C E_C} + \frac{1.13}{A_S E_S}\right) - 0.015 \tag{53}$$

The second failure mode is that the internal force of bar *AD* exceeds its ultimate stress. The internal force of bar *AD* is $N_{AD} = 1.35ql$, and the ultimate strength of the bar is $f_C A_C$, where f_C is the compressive stress of the bar. The second limit-state function is given by

$$g_2(\mathbf{X}) = 1.185ql - f_C A_C \tag{54}$$

A failure occurs when the internal force of bar *EC* $N_{EC} = 1.3ql$ exceeds its ultimate stress $f_S A_S$, where f_S is the tensile strength of the bar. Therefore, the third limit-state function is formulated by

$$g_3(\mathbf{X}) = 0.65ql - f_S A_S \tag{55}$$

E_C and E_S are lognormally distributed, and the rest of random variables q, l, A_S, A_C, f_C, and f_C are normally distributed. They are listed in Table 3.

Table 3 Distribution of random variables

Place Table 3 here

After the MPPs are found, the reliability indexes and directional vectors are available.

$$\beta_1 = 4.6396$$

$$\beta_2 = 3.8122$$

$$\beta_3 = 3.4440$$

$$\boldsymbol{\alpha}_1 = (0.7054, 0.1857, -0.4890, -0.2122, -0.4147, -0.1465, 0, 0)$$

$$\boldsymbol{\alpha}_2 = (0.1686, 0.0179, 0, -0.1504, 0, 0, 0, -0.9740)$$

$$\boldsymbol{\alpha}_3 = (0.2009, 0.0215, -0.1325, 0, 0, 0, -0.9704, 0)$$

Similarly, the reliability of each component is calculated by the second-order SPA, which produces $R_1 = 1.0$, $R_2 = 0.9999$, and $R_3 = 0.9997$. The mean values of the three equivalent component responses $\mathbf{Z} = (Z_1, Z_2, Z_3)$ are then calculated by

$$\boldsymbol{\mu}_Z = \boldsymbol{\beta}^{\mathrm{SPA}} = (\beta_i^{\mathrm{SPA}})_{i=1,2,3} = \Phi^{-1}(R_i)_{i=1,2,3} = (4.5985, 3.7999, 3.4358)$$

The covariance matrix $\boldsymbol{\Sigma}_Z$ is

$$\boldsymbol{\Sigma}_Z = \begin{bmatrix} 1 & \rho_{12} & \rho_{13} \\ \rho_{21} & 1 & \rho_{23} \\ \rho_{31} & \rho_{32} & 1 \end{bmatrix} = \begin{bmatrix} 1 & 0.1542 & 0.2092 \\ 0.1542 & 1 & 0.0343 \\ 0.2092 & 0.0343 & 1 \end{bmatrix}$$

Thus, the system probability of failure is estimated to be $p_{Sf} = 3.6983 \times 10^{-4}$.

When FORM is used, the covariance matrix remains the same, and the mean values of the three equivalent component responses are $\boldsymbol{\mu}_Z = (4.6396,\ 3.8122,\ 3.4440)$. Based on Eq. (38), the system probability of failure is $p_{Sf} = 3.5714\times10^{-4}$. Similarly, the system probability of SORM is $p_{Sf} = 3.6642\times10^{-4}$. The solution from MCS with a sample size of 1×10^{7} serves as a benchmark for the accuracy comparison. All results are given in Table 4, which indicates that SOSPA is more accurate than FORM and SORM while the latter is more efficient than the former.

Table 4 Probability of system failure in Example 2

Place Table 4 here

4.3 Example 3

This example has ten polynomial surface response functions used as a surrogate for a more computationally intensive numerical model of the various phenomena leading to failure [31, 32]. The system reliability is defined by

$$R_{Sf} = \Pr(g_1(\mathbf{X}) \le 0 \cap g_2(\mathbf{X}) \le 0 \cap ... \cap g_9(\mathbf{X}) \le 0 \cap g_{10}(\mathbf{X}) \le 0) \tag{56}$$

The limit-state functions $g_i(\cdot)$ are given below.

$$g_1(\mathbf{X}) = 1.16 - 0.3717X_2X_4 - 0.00931X_2X_{10} - 0.484X_3X_9 + 0.01343X_6X_{10} - 1 \tag{57}$$

$$\begin{aligned} g_2(\mathbf{X}) = 4.72 - 0.5X_4 - 0.19X_2X_3 - 0.0122X_4X_{10} \\ + 0.009325X_6X_{10} + 0.000191X_{11}^2 - 4.01 \end{aligned} \tag{58}$$

$$\begin{aligned} g_3(\mathbf{X}) = 28.98 + 3.818X_3 - 4.2X_1X_2 + 0.0207X_5X_{10} + 6.63X_6X_9 \\ - 7.7X_7X_8 + 0.32X_9X_{10} - 32 \end{aligned} \tag{59}$$

$$g_4(\mathbf{X}) = 33.86 + 2.95X_3 + 0.1792X_{10} - 5.057X_1X_2 - 11X_2X_8 - 0.0215X_5X_{10} - 9.98X_7X_8 - 22X_8X_9 - 32 \quad (60)$$

$$g_5(\mathbf{X}) = 46.36 - 9.9X_2 - 12.9X_1X_8 + 0.1107X_3X_{10} - 32 \quad (61)$$

$$g_6(\mathbf{X}) = 0.261 - 0.0159X_1X_2 - 0.188X_1X_8 - 0.019X_2X_7 + 0.0144X_3X_5 + 0.0008757X_5X_{10} - 0.32 \quad (62)$$

$$g_7(\mathbf{X}) = 0.214 + 0.00817X_5 - 0.131X_1X_8 - 0.0704X_1X_9 + 0.03099X_2X_6 - 0.018X_2X_7 + 0.0208X_3X_8 + 0.121X_3X_9 - 0.00364X_5X_6 + 0.0007715X_5X_{10} - 0.0005354X_6X_{10} + 0.00121X_8X_{11} - 0.32 \quad (63)$$

$$g_8(\mathbf{X}) = 0.74 - 0.61X_2 - 0.163X_3X_8 + 0.001232X_3X_{10} - 0.166X_7X_9 + 0.227X_2^2 - 32 \quad (64)$$

$$g_9(\mathbf{X}) = 10.58 - 0.674X_1X_2 - 1.95X_2X_8 + 0.02054X_3X_{10} - 0.0198X_4X_{10} + 0.028X_6X_{10} - 9.9 \quad (65)$$

$$g_{10}(\mathbf{X}) = 16.45 - 0.489X_3X_7 - 0.843X_5X_6 + 0.0432X_9X_{10} - 0.0556X_9X_{11} - 0.0003X_{11}^2 - 15.69 \quad (66)$$

There are eleven random variables which are B-pillar inner (X_1), B-pillar reinforcement (X_2), floor side inner (X_3), cross members (X_4), door beam (X_5), door belt line reinforcement (X_6), roof rail (X_7), B-pillar inner (X_8), floor side inner (X_9), barrier height (X_{10}), and barrier hitting position (X_{11}). All of them are normally distributed with parameters defined in the Table 5.

The reliability indexes of all components are at first calculated by FORM, which yields $\beta_1 = 9.3064$, $\beta_2 = 1.8772$, $\beta_3 = 4.0596$, $\beta_4 = 2.9767$, $\beta_5 = 1.2968$, $\beta_6 = 12.1197$, $\beta_7 = 15.5223$, $\beta_8 = 4.8357$, $\beta_9 = 3.7118$ and $\beta_{10} = 1.8782$. Therefore, for FORM, the mean values of ten equivalent component responses $\mathbf{Z} = (Z_1, Z_2, \cdots, Z_{10})$ are

$$\boldsymbol{\mu}_Z = (9.3064, 1.8772, 4.0596, 2.9767, 1.2968, 12.1197, 15.5223, 4.8357, 3.7118, 1.8782)$$

The 10-by-10 covariance matrix is given by

$$\boldsymbol{\Sigma}_Z = \begin{bmatrix} 1 & -0.7651 & \cdots & 0.9021 & 0.5581 \\ -0.7651 & 1 & \cdots & -0.9285 & -0.7498 \\ \vdots & \vdots & \ddots & \vdots & \vdots \\ 0.9021 & -0.9285 & \cdots & 1 & 0.7093 \\ 0.5581 & -0.7498 & \cdots & 0.7093 & 1 \end{bmatrix}_{10\times 10}$$

The system probability of failure from FORM method is $p_{Sf} = 1 - R_S = 0.1390$.

When SOSPA method is used, the mean values of the ten equivalent component responses are given by

$$\boldsymbol{\mu}_Z^{\text{SPA}} = (9.3286, 1.4495, 4.0629, 2.9759, 1.2983, 12.1274, 15.4725, 4.8079, 3.7234, 2.0335)$$

Table 5 Distribution of random variables

Place Table 5 here

The probability of system probability from SOSPA is then given by $p_{Sf} = 0.1777$.

All results are given in Table 6, which also indicates that SOSPA is much more accurate than FORM and SORM while the latter is more efficient than the former. For this problem with 10 responses, the error from FORM and SORM are too large.

Table 6 Probability of system failure in Example 3

Place Table 6 here

4.4 Example 4

The final example involves an assembly system where a rectangular steel bar cantilevered to a steel channel with four identical tightly fitted bolts located at points *A*, *B*, *C*, and *D* as shown in Fig. 1. The rectangular bar is subjected to an external force *F*. All random variables are given in Table 7.

Place Figure 1 here

Fig. 1 A cantilever bar

Table 7 Distribution of random variables

Place Table 7 here

The centroid of the bolt group *O* is found by symmetry. The shear reaction V passes through *O*, and the moment reaction M is about *O*. They are given by $V = F$, $M = F(l_1 + l_2 + \frac{l_4}{2})$. The distance from the centroid to the center of each bolt is

$$r = 0.5\sqrt{l_4^2 + l_5^2}$$

The primary shear load per bolt is $F' = \frac{V}{4}$. Since the secondary shear forces are equal, they become $F'' = \frac{Mr}{4r^2} = \frac{M}{4r}$. The resultants of the primary and secondary shear forces are obtained by using the parallelogram rule. The magnitudes are found to be

$$F_A = F_B = \sqrt{(F')^2 + (F'')^2 - 2F'F''cos\theta_1}$$

$$F_C = F_D = \sqrt{(F')^2 + (F'')^2 - 2F'F''cos\theta_2}$$

where $\theta_1 = \frac{pi}{2} + \arctan\left(\frac{l_4}{l_5}\right)$, and $\theta_2 = \frac{pi}{2} - \arctan\left(\frac{l_4}{l_5}\right)$.

The largest bearing stress is due to the pressing of the bolt against the channel web. The bearing area of the channel is $A_1 = t_1 d_a$. The maximum bearing stress of the channel should be smaller than its yield strength, which is given by

$$g_1(\mathbf{X}) = \frac{F_A}{A_1} - S_1 \quad (67)$$

Correspondingly, the limit-state function of the bar is defined by

$$g_2(\mathbf{X}) = \frac{F_A}{A_2} - S_2 \quad (68)$$

where $A_2 = t_2 d_a$

The critical bending stress in the bar occurs at the cross section *A-B*, where the bending moment is $M_1 = F(l_1 + l_2)$. The second moment of area of the section is

$$I = I_{bar} - 2\left(I_{holes} + \bar{d}^2 A\right) = \frac{t_2 l_2^3}{12} - 2\left[\frac{t_2 d_a^3}{12} + \frac{l_5^2}{4} t_2 d_a\right]$$

The bending stress of the bar should be smaller than its yield strength, and this is given by

$$g_3(\mathbf{X}) = \frac{M_1}{I/c} - S_2 \quad (69)$$

where I/c is the section modulus for the bar, $c = l_3/2$.

Bolt *A* and *B* are critical because they carry the largest shear load F_A and F_B. The shear stress of the bolts should not be greater than the allowable shear stress. Thus, the limit-state functions of bolts *A* and *B* are defined by

$$g_4(\mathbf{X}) = \frac{F_A}{A_{sa}} - \tau_a \tag{70}$$

$$g_5(\mathbf{X}) = \frac{F_B}{A_{sb}} - \tau_b \tag{71}$$

where A_{sa} and A_{sb} are shear-stress areas.

Similarly, the limit-state functions of bolts *C* and *D* are defined by

$$g_6(\mathbf{X}) = \frac{F_C}{A_{sc}} - \tau_c \tag{72}$$

$$g_7(\mathbf{X}) = \frac{F_D}{A_{sd}} - \tau_d \tag{73}$$

where A_{sc} and A_{sd} are shear-stress areas.

There are seven limit-state functions. The system probabilities of failure and the function calls from all methods are provided in Table 8. The results show that SOSPA is the most accurate method because its error is only 0.593% compared with the MCS result and the errors of SORM and FORM are much larger. FORM is the most efficient method since its number of function calls is the least. SOSPA and SORM call the limit-state functions with the same time.

Table 8 Probability of system failure in Example 4

Place Table 8 here

----

5. CONCLUSION

The proposed second order saddlepoint approximation (SOSPA) method is an alternative method for system reliability analysis. This method results in higher accuracy than the first order approximation method by combing the second order approximation and saddlepoint approximation. SOSPA accurately produces the marginal distributions of all component responses. This is achieved by employing the saddlepoint approximation after transforming the approximated second-order limit-state functions into linear combinations of noncentral chi-square variables. The dependences between component responses are considered with the only first approximation for the sake of efficiency. With the estimated marginal component distributions and component correlations, the joint distribution of all the component responses is formed by a multivariate normal distribution, which leads to a fast evaluation of the system reliability.

The accuracy of the proposed is largely determined by the accuracy of the approximated limit-state functions with second order Taylor expansion in the vicinity of the most probable points. The accuracy is also affected by the first order approximation for estimating correlations between component responses.

How to more accurately estimate component correlations by a second order approximation needs a further investigation. The other future work is to incorporate the system reliability analysis in reliability-based design optimization.

ACKNOWLEDGEMENTS

The authors wound like to gratefully acknowledge the support from the National Science Foundation under Grant Numbers CMMI 1923799 and CMMI 1924413.

REFERENCES

[1] Hu, Z. and Du, X., 2014, "Lifetime cost optimization with time-dependent reliability," Engineering Optimization, 46(10), pp. 1389-1410.
[2] Rausand, M., and Høyland, A., 2004, System reliability theory: models, statistical methods, and applications, John Wiley & Sons.
[3] Ditlevsen, O., 1979, "Narrow reliability bounds for structural systems," Journal of structural mechanics, 7(4), pp. 453-472.
[4] Song, J., and Der Kiureghian, A., 2003, "Bounds on system reliability by linear programming," Journal of Engineering Mechanics 129(6), pp. 627-636.
[5] Youn, B. D., and Wang, P., 2009, "Complementary intersection method for system reliability analysis," Journal of Mechanical Design, 131(4), p. 041004.
[6] Du, X., 2010, "System reliability analysis with saddlepoint approximation," Structural and Multidisciplinary Optimization, 42(2), pp. 193-208.
[7] Kang, W. H., Song, J. and Gardoni, P., 2008, "Matrix-based system reliability method and applications to bridge networks," Reliability Engineering & System Safety, 93(11), pp. 1584-1593.
[8] Hu, C. and Youn, B. D., 2011, "Adaptive-sparse polynomial chaos expansion for reliability analysis and design of complex engineering systems," Structural and Multidisciplinary Optimization, 43(3), pp. 419-442.
[9] Rocco, C. M. and Moreno, J. A., 2002, "Fast Monte Carlo reliability evaluation using support vector machine," Reliability Engineering & System Safety, 76(3), pp. 237-243.
[10] Bichon, B., Eldred, M., Swiler, L., Mahadevan, S., and McFarland, J., 2007, "Multimodal reliability assessment for complex engineering applications using efficient global optimization," AIAA Paper, No. AIAA-2007-1946.
[11] Bichon, B. J., McFarland, J. M., and Mahadevan, S., 2011, "Efficient surrogate models for reliability analysis of systems with multiple failure modes," Reliability Engineering and System Safety, 96(10), pp. 1386-1395.
[12] Fauriat, W., and Gayton, N., 2014, "AK-SYS: An adaptation of the AK-MCS method for system reliability," Reliability Engineering and System Safety, 123, pp. 137-144.
[13] Wu, H., Zhu, Z., and Du, X., 2020, "System Reliability Analysis with Autocorrelated Kriging Predictions," Journal of Mechanical Design, pp.1-42.
[14] Madsen, H. O., Krenk, S., and Lind, N. C., 2006, Methods of structural safety, Courier Corporation.

[15] Du, X., and Sudjianto, A., 2004, "First order saddlepoint approximation for reliability analysis," AIAA Journal , 42(6), pp. 1199-1207.
[16] Der Kiureghian, A., and Dakessian, T., 1998, "Multiple design points in first and second-order reliability," Structural Safety, 20(1), pp. 37-49.
[17] Madsen, H., 1985, "First order vs. second order reliability analysis of series structures," Structural Safety, 2(3), pp. 207-214.
[18] Du, X., 2008, "Saddlepoint approximation for sequential optimization and reliability analysis," Journal of Mechanical Design, 130(1), p. 011011.
[19] Hohenbichler, M., and Rackwitz, R., 1982, "First-order concepts in system reliability," Structural Safety, 1(3), pp. 177-188.
[20] Hu, Z., and Du, X., 2018, "Saddlepoint approximation reliability method for quadratic functions in normal variables," Structural Safety, 71, pp. 24-32.
[21] Papadimitriou, D. I., Mourelatos, Z. P., and Hu, Z., 2018, "Reliability Analysis Using Second-Order Saddlepoint Approximation and Mixture Distributions," Journal of Mechanical Design, 141(2), p. 021401
[22] Der Kiureghian, A., Lin, H.Z., and Hwang, S., 1987, "Second-order reliability approximations," Journal of Engineering mechanics, 113(8), pp. 1208-1225.
[23] Konishi, S., Niki, N., and Gupta, A., 1988, "Asymptotic expansions for the distribution of quadratic forms in normal variables," Annals of the Institute of Statistical Mathematics , 40(2), pp. 279-296.
[24] Tanizaki, H., 2004, Computational methods in statistics and econometrics, CRC Press.
[25] Lugannani, R., and Rice, S., 1980, "Saddle point approximation for the distribution of the sum of independent random variables," Advances in applied probability, 12(2), pp. 475-490.
[26] Zeng, P., Jimenez, R., Li, T., Chen, Y., and Feng, X., 2017, "Application of Quasi-Newton Approximation-Based SORM for System Reliability Analysis of a Layered Soil Slope," Geo-Risk 2017, pp. 111-119.
[27] Gollwitzer, S., and Rackwitz, R., 1988, "An efficient numerical solution to the multinormal integral," Probabilistic Engineering Mechanics, 3(2), pp. 98-101.
[28] Pandey, M., 1998, "An effective approximation to evaluate multinormal integrals," Structural safety, 20(1), pp. 51-67.
[29] Genz, A., 1992, "Numerical computation of multivariate normal probabilities," Journal of computational and graphical statistics, 1(2), pp. 141-149.
[30] Wei, P., Liu, F. and Tang, C., 2018, "Reliability and reliability-based importance analysis of structural systems using multiple response Gaussian process model," Reliability Engineering & System Safety, 175, pp. 183-195.
[31] Du, X., and Chen, W., 2004, "Sequential Optimization and Reliability Assessment Method for Efficient Probabilistic Design," Journal of Mechanical Design, 126(2), pp. 225-233.

[32] Gu, L., Yang, R. J., Tho, C. H., Makowskit, M., Faruquet, O., and Y.Li Y.Li, 2001, "Optimisation and robustness for crashworthiness of side impact," International Journal of Vehicle Design, 26(4), pp. 348-360.

List of Table Captions

List of Figure Captions

Table 1 MPP, reliability index and directional vector

	$\mathbf{u}^*$	β	$\boldsymbol{\alpha}$
g_1	(-2.6981,-2.0057)	3.3602	(0.8025,0.5966)
g_2	(-2.5485, 1.8429)	3.1450	(0.8103,-0.5869)

Table 2 Probability of system failure in Example 1

Method	p_{Sf}	ε (%)	Total function calls
SOSPA	1.0702×10^{-3}	0.29	45
SORM	1.0878×10^{-3}	1.35	45
FORM	1.2111×10^{-3}	12.80	39
MCS	1.0733×10^{-3}	N/A	10^7

Table 3 Distribution of random variables

	Variables	Distribution
X_1	q (N/m)	N(14000,1400)
X_2	L (m)	N(12, 0.12)
X_3	A_S (m^2)	$\mathrm{N}(9.00\times10^{-4}, 0.54\times10^{-4})$
X_4	A_C (m^2)	$\mathrm{N}(5\times10^{-2}, 4\times10^{-3})$
X_5	E_S (N/m^2)	$\mathrm{LN}(2\times10^{11}, 0.12\times10^{11})$
X_6	E_C (N/m^2)	$\mathrm{LN}(3\times10^{11}, 0.18\times10^{11})$
X_7	f_S (N/m^2)	$\mathrm{N}(3.35\times10^{8}, 0.60\times10^{8})$
X_8	f_C (N/m^2)	$\mathrm{N}(1.34\times10^{7}, 0.24\times10^{7})$

Table 4 Probability of system failure in Example 2

Method	p_{Sf}	ε (%)	Total function calls
SOSPA	3.6983×10^{-4}	0.34	243
SORM	3.6642×10^{-4}	1.26	243
FORM	3.5714×10^{-4}	3.76	135
MCS	3.7110×10^{-4}	N/A	10^{7}

Table 5 Distribution of random variables

Random variable	Distribution
X_1 (mm)	N(0.500,0.030)
X_2 (mm)	N(1.310,0.030)
X_3 (mm)	N(0.500,0.030)
X_4 (mm)	N(1.395,0.030)
X_5 (mm)	N(0.875,0.030)
X_6 (mm)	N(1.200,0.030)
X_7 (mm)	N(0.400,0.030)
X_8 (GPa)	N(0.345,0.006)
X_9 (GPa)	N(0.192,0.006)
X_{10} (mm)	N(0.0,10.0)
X_{11} (mm)	N(0.0,10.0)

Table 6 Probability of system failure in Example 3

Method	p_{Sf}	ε(%)	Total function calls
SOSPA	0.1777	3.31	1572
SORM	0.1355	26.40	1572
FORM	0.1391	24.30	912
MCS	0.1838	N/A	10^7

Table 7 Distribution of random variables

	Variables	Distribution
X_1	F (N)	$\mathrm{N}(1.6 \times 10^4, 1.6 \times 10^3)$
X_2	S_1 (Pa)	$\mathrm{LN}(300 \times 10^6, 57 \times 10^6)$
X_3	S_2 (Pa)	$\mathrm{LN}(300 \times 10^6, 57 \times 10^6)$
X_4	τ_a (Pa)	$\mathrm{LN}(310 \times 10^6, 59 \times 10^6)$
X_5	τ_b (Pa)	$\mathrm{LN}(310 \times 10^6, 59 \times 10^6)$
X_6	τ_c (Pa)	$\mathrm{LN}(310 \times 10^6, 59 \times 10^6)$
X_7	τ_d (Pa)	$\mathrm{LN}(310 \times 10^6, 59 \times 10^6)$
X_8	t_1 (m)	$\mathrm{N}(1.0 \times 10^{-2}, 2.0 \times 10^{-4})$
X_9	t_2 (m)	$\mathrm{N}(1.0 \times 10^{-2}, 2.0 \times 10^{-4})$
X_{10}	d_a (m)	$\mathrm{N}(1.6 \times 10^{-2}, 3.2 \times 10^{-4})$
X_{11}	d_b (m)	$\mathrm{N}(1.6 \times 10^{-2}, 3.2 \times 10^{-4})$
X_{12}	d_c (m)	$\mathrm{N}(1.6 \times 10^{-2}, 3.2 \times 10^{-4})$
X_{13}	d_d (m)	$\mathrm{N}(1.6 \times 10^{-2}, 3.2 \times 10^{-4})$
X_{14}	l_1 (m)	$\mathrm{N}(3.2 \times 10^{-1}, 6.4 \times 10^{-3})$
X_{15}	l_2 (m)	$\mathrm{N}(5.0 \times 10^{-2}, 1.0 \times 10^{-3})$
X_{16}	l_3 (m)	$\mathrm{N}(2.0 \times 10^{-1}, 4.0 \times 10^{-3})$
X_{17}	l_4 (m)	$\mathrm{N}(1.5 \times 10^{-1}, 3.0 \times 10^{-3})$
X_{18}	l_5 (m)	$\mathrm{N}(1.2 \times 10^{-2}, 2.4 \times 10^{-3})$
X_{19}	A_{sa} (m^2)	$\mathrm{N}(1.44 \times 10^{-4}, 2.88 \times 10^{-6})$
X_{20}	A_{sb} (m^2)	$\mathrm{N}(1.44 \times 10^{-4}, 2.88 \times 10^{-6})$
X_{21}	A_{sc} (m^2)	$\mathrm{N}(1.44 \times 10^{-4}, 2.88 \times 10^{-6})$

X_{22}	A_{sd} (m^2)	$\mathrm{N}(1.44 \times 10^{-4}, 2.88 \times 10^{-6})$

Table 8 Probability of system failure in Example 4

Method	p_{Sf}	ε (%)	Total function calls
SOSPA	1.1672×10^{-3}	1.71	2599
SORM	1.0273×10^{-3}	13.50	2599
FORM	1.2292×10^{-3}	3.51	828
MCS	1.1875×10^{-3}	N/A	10^7

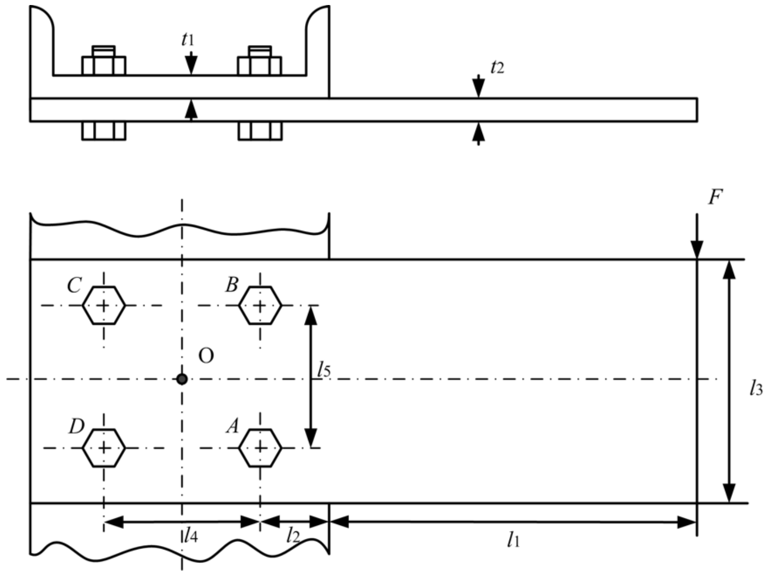

Fig. 1 A cantilever bar